Microvascular Changes in Lymph Nodes Draining Skin Allografts

Norman D. Anderson, MD, Arthur O. Anderson, MD, and Robert G. Wyllie, MD

Histologic, histochemical, ultrastructural, and radiolabeling characteristics of the microvasculature in regional nodes draining skin allograft sites are described. From 12 to 48 hours after grafting, these nodes show increased vascular permeability and altered lymphocyte traffic pattern. The rapid rise in lymphocyte migration indices and the apparent plugging of intermediate sinuses by lymphocytes suggest that both increased entry and decreased egress of recirculating cells contribute in "lymphocyte trapping." This is followed by redistribution of cortical capillary arcades as existing germinal centers dissolve and proliferating lymphocytes infiltrate the cortex. Normal microvascular patterns reappeared at 7 to 14 days as primary and secondary nodules form in the enlarged nodes. Increased length and arborization of high endothelial venules resulted from focal proliferation of endothelial cells in transition zones from high to low endothelium. In stimulated nodes, high endothelial cells exhibit increased cytoplasmic basophilia and acid hydrolase activities which correlate with the appearance of numerous polyribosomes, RER cisternae, and lysosomes in their cytoplasm. These "activated" endothelial cells phagocytose microthrombi within venular lumens. (Am J Pathol 81:131–160, 1975)

PREVIOUS STUDIES have established that the microcirculation provides for the nutrition, fluid exchange, and cellular traffic in lymphatic tissue.[1,2] However, there is only fragmentary knowledge of the microvascular changes in antigen-stimulated nodes which undergo rapid enlargement due to the combined effects of inflammation,[3] cellular trapping,[4] and lymphocytic proliferation.[5] Repeated histologic demonstrations of hyperemia, edema, fibrin exudates, extravasated blood, and particle leakage clearly indicated that vascular permeability was altered in stimulated nodes.[6] Several investigators have suggested that blood vessels in the outer cortical lobules might be displaced and remodeled as secondary nodules formed in the response to antigenic stimulation,[7,8] but extensive changes in the nodal vasculature were considered unlikely.[9] This concept of a rather static vasculature has been challenged by recent studies by Herman *et al.*,[10] who described complete dissolution and gradual reforma-

From the Departments of Medicine, Pathology, and Surgery, The Johns Hopkins Medical Institutions, Baltimore, Maryland.

Supported in part by Grants HL-17569 and GM-00415 from the National Institutes of Health and by a grant from the Maryland Division of the American Cancer Society.

Accepted for publication June 9, 1975.

Address reprint requests to Dr. Norman D. Anderson, Departments of Medicine and Surgery, The Johns Hopkins University School of Medicine, Baltimore, MD 21205.

tion of the vascular units in the lymph node cortex at sequential stages after antigenic challenge.

Since recirculating lymphocytes leave the blood stream and enter lymphatic tissues by emigrating selectively across the walls of high endothelial venules (HEV),[2] there has been considerable interest in determining whether these specialized venules were altered in stimulated nodes. Burwell [11] described increased cytoplasmic basophilia in HEV of regional nodes draining allografts, but the significance of these changes is still unknown. Several investigators postulated that HEV might proliferate following antigenic stimulation,[11,12] but this has never been adequately documented.[10] Mitotic figures have been reported to be rare in endothelial cells [14,15] and radiolabeling studies have shown slow cell turnover in HEV.[16]

In the present study, light microscopic, histochemical, ultrastructural, and radioautographic techniques were employed to characterize sequential changes in the microvasculature of regional nodes draining skin allografts. Results indicated that altered permeability, remodeling, and focal endothelial proliferation occurred in the blood vessels within stimulated nodes. These changes were accompanied by a transient increase in lymphocyte traffic across the walls of HEV, trapping of lymphocytes within sinuses, and lymphocyte proliferation in the cortex. Many high endothelial cells exhibited metabolic and ultrastructural changes of "activation" which correlated with phagocytic functions of these cells.

Materials and Methods

Animals

Adult male Lewis (Le) and Brown Norway (BN) rats (Microbiological Associates, Walkersville, Md.) weighing between 190 to 250 were used in this study.

Anesthesia

Rats were anesthetized for all surgical procedures by intraperitoneal injections with aqueous solutions of chloral hydrate at dosages of 360 mg/kg body weight.

Skin Grafting Techniques

Full-thickness BN skin grafts were placed into beds prepared on the lateral thoracic walls of 60 Le rats using standard grafting techniques.[17] The draining and contralateral axillary nodes were excised for study on days 1 through 4, 7, 14 and 28. Skin grafts between these inbred strains crossed major histocompatibility loci (Le = AgB_1; BN = AgB_3) [18] and were routinely destroyed within 11 days.

Regional Perfusion Techniques

The axillary node microvasculature was stained *in vivo* in 4 rats at each designated interval by infusing 0.4 ml of 2% alcian blue dye (8GS; Schmid & Co., Stuttgart, Germany) into

their brachial arteries. These nodes were excised, fixed in glutaraldehyde, cleared in dimethyl sulfoxide, and examined as whole mount preparations using methods reported previously.[19]

Preparation of Tissue Samples

Four additional grafted rats were killed by cervical dislocation at each time interval. The draining and contralateral axillary nodes were excised, trimmed from adventitial fat, and bisected. One half of each specimen was snap-frozen in liquid nitrogen, and 4-μ cryostat sections were cut for histochemical studies. The remaining halves were prepared for electron microscopy using techniques described in that section.

Histochemistry

Cryostat sections were dried in a vacuum for 10 minutes before staining. The following tissue components were stained, using previously described methods: lactic and isocitric acid dehydrogenase,[20] RNA,[21] adenosine triphosphatase,[22] acetyl esterase,[23] acid phosphatase,[24] β-glucuronidase,[25] and elastic tissue.[26]

Electron Microscopic Techniques

Portions of each lymph node were minced into 1-mm cubes in a drop of cold 3% glutaraldehyde in 0.1 M cacodylate buffer at pH 7.2 and placed in fresh fixative for 2 to 4 hours at 4 C. After washing overnight in 3% sucrose in 0.1 M cacodylate, fragments were postfixed in 1% osmium tetroxide in Millonig's buffer at pH 7.2; tissue slices were washed in 70% alcohol, dehydrated through graded alcohols to toluene, and embedded in araldite. Thick sections (0.5 to 1.0 μ were cut with glass knives on a Sorvall MT-1 and stained with toluidine blue. Thin sections were cut at 0.006 to 0.009 μ with diamond knives on a Sorval MT-2 ultramicrotome and mounted on uncoated 200-mesh copper grids which were stained with aqueous uranyl acetate and/or lead citrate and examined at magnifications ranging from 1,600 to 16,000 on an AEI 801 electron microscope.

Radiolabeling Techniques

Three days after grafting with BN skin, Le rats were placed in restraining cages and continuously infused with saline containing ^{3}H-thymidine (specific activity, 15.8 Ci/mole; New England Nuclear, Boston, Mass.) at a dose of 0.5 μCi/g body wt/24 hours for 72 hours. Rats were killed by cervical dislocation; regional axillary and contralateral inguinal nodes were excised and fixed in 10% buffered formalin; 6-μ sections were processed for autoradiography using HTB-2 liquid emulsion (Eastman-Kodak, Rochester, N.Y.). Sections were exposed for 8 to 14 weeks and stained through the emulsion with hematoxylin and eosin.

Results

Changes in Axillary Node Weight

Axillary weights were recorded to provide an index for relating microvascular changes to nodal size. Sequential changes in nodal weight observed in 56 Le rats after grafting with BN skin (Table 1) demonstrated a significant increase in axillary node weight within 2 days after grafting. Stimulated nodes then rapidly increased in size to reach their maximal weights at 1 week, and showed only slight reduction in size over the remaining 1 month.

Table 1—Changes in Axillary Node Weight Following Skin Grafting (8 rats/group)

Day after grafting	Axillary node weight (mg wet tissue)	
	Mean	Range
0	18.0	14–20
1	21.0	17–24
2	25.5	19–31
3	28.5	25–33
4	29.8	27–34
7	43.5	35–51
14	38.5	33–43
28	37.8	30–44

Microvasculature of Axillary Lymph Nodes

Regional perfusions with alcian blue dye stained luminal surfaces of the vascular endothelium in all lymph node vessels. The microvasculature was studied by microscopic examination of cleared, serial 150-μ tissue slices prepared from each node. Arteries, capillaries, HEV, and veins were identified readily in these preparations by their characteristic staining patterns, vascular connections, and luminal size. The microvasculature patterns in draining and contralateral axillary nodes were compared in each animal.

Microvascular Patterns of Contralateral Nodes

All of the 28 contralateral nodes examined showed similar vascular patterns and were identical to those seen in normal adult Lewis rats (Figure 1). The major artery entering the lymph node hilus divided into small branches which passed longitudinally through the medulla. These arteries had small side branches which supplied the medullary cords, and larger branches which vertically entered lobules of cortical lymphatic tissue situated between fibrous trabeculae. Two or three small arteries passed through the periphery of each lobule and continued branching until they terminated in the subcapsular capillary bed. Within the cortex, germinal centers were easily identified as relatively avascular nodules (containing only a central metarteriole and occasional capillaries), surrounded by a meshwork of arterioles, capillaries, and small veins. Dense arcades of anastomosing capillaries were seen beneath the subcapsular sinus and surrounding medullary cords. A less prominent capillary network was dispersed throughout the deep cortex. Cortical capillaries drained into small venules lined by flat endothelium which joined with HEV. Numerous arteriovenous communications (AVC) looped through the outer cortical arcade and anastomosed with these small venules. Each cortical lobule was drained by two to three major venous trunks lined by high en-

dothelium. These HEV received three to five short side branches lined with high endothelial cells and several venules lined with flat endothelium. The arborizing HEV were distributed randomly in cortical lobules. These HEV drained centripetally toward the medulla where they merged into segmental veins lined with flat endothelium. Venous sphincters in varying degrees of constriction were occasionally seen at junctions between segmental veins or at sites where these veins joined with larger efferent vessels near the hilus.

Microvascular Patterns in Draining Lymph Nodes

Regional nodes draining skin allografts showed a definite sequence of vascular changes. While there were some variations in the onset and extent of these alterations between individual animals, the following descriptions present a composite view of the microvascular patterns observed in axillary nodes from 4 rats at each designated time interval.

One Day

Dilated AVC and prominent subcapsular capillary arcades were seen in all nodes within 24 hours. Numerous venous constrictions were observed, and this was paralleled by an increase in the average luminal diameter of segmental veins to 70 μ in contralateral nodes. Alcian blue infusions caused diffuse staining of nodal reticular fibers consistent with altered vascular permeability. No significant alterations were observed in other blood vessels; secondary nodules were still recognizable in the cortex.

Two Days

Prominent AVC, dilated cortical capillaries, focal venous constrictions, and venous engorgement were observed in each node. Intraarterial infusions with alcian blue caused diffuse reticular fiber staining, and three nodes showed frank extravasation of dye and erythrocytes into the subcapsular and medullary sinuses.

Three Days

The cortex was wider, causing displacement and compression of the medullary vasculature. A rich network of dilated capillaries was evenly distributed through the cortex. Avascular germinal centers could not be identified. In subcapsular regions, AVC were less prominent but numerous dilated arteriovenous shunts were seen in the deep cortex. The main trunks of HEV appeared to be oriented vertically as they penetrated the cortex (Figure 2). These venules received four to seven side branches and each was lined by short segments of high endothelium. Alcian blue

infusions caused faint, irregular staining of reticular fibers. Venous constrictions were not seen, and luminal diameters in segmental veins measured 40 to 50 μ.

Four Days

In these nodes the cortex was markedly widened and contained a dilated network of randomly distributed capillaries. No avascular germinal centers were seen. Small glomerulus-like capillary tufts formed about primary nodules in the deep cortex. HEV retained their vertical orientation in the cortex; side branches exhibited relatively long segments lined by high endothelium which formed a freely communicating venous plexus. Prominent AVC were observed in the deep cortex. Although most medullary vessels appeared compressed by the expanding cortex, rich capillary arcades surrounding medullary cords were dilated. The segmental veins appeared normal; no contracted venous sphincters were seen.

Seven Days

The lymph node cortices had reached their maximal thickness by 1 week. Branching capillary arcades of normal caliber were evenly distributed throughout the cortex. Small, relatively avascular secondary nodules were occasionally seen in the deep cortex. HEV were randomly oriented as they followed a tortuous course across the cortex. All side branches from these venules were lined by high endothelial cells (Figure 3). These branches extended 100 to 450 μ into the adjacent cortex and linked directly with short segments of small venules lined with flat endothelium. Dilated capillary arcades were seen about compressed medullary cords. No signs of altered vascular permeability or venous dilatation were observed.

Fourteen Days

Although nodal enlargement persisted, the microvasculature appeared to be reverting towards a normal pattern at 2 weeks. The cortex appeared slightly thinner and contained several large germinal centers. These relatively avascular structures displaced and compressed adjacent capillary arcades. Long, narrow AVC appeared to be stretched as they passed over the secondary nodules and anastomosed directly with venules lined with high endothelium. Arborizing HEV extended from beneath the subcapsular sinus to the corticomedullary junction in each cortical lobule. Long segments of the branches extending from these vessels had relatively large lumens surrounded by high endothelium. Medullary cords were enlarged and encircled by a rich meshwork of dilated capillaries.

Twenty-eight Days

All lymph nodes examined at 4 weeks remained enlarged and showed the same general vascular pattern noted at 14 days.

Histologic Changes in Draining Lymph Nodes

One-micron sections from 28 nodes were examined by light microscopy for signs of vascular changes, altered lymphocyte traffic, and cellular proliferation which might correlate with variations observed in microvascular patterns (Table 2). Distinctive histologic changes occurred in all regional nodes shortly after grafting. From 12 to 48 hours, numerous erythrocytes were seen within subcapsular and medullary sinuses, where they were being phagocytosed by macrophages and littoral cells. Occasional granulocytes were also present in these sinuses. These findings probably reflected inflammatory changes induced by surgical grafting procedures, since comparable alterations were not seen in contralateral nodes. Several nodes examined at 48 hours showed extravasation of blood cells from venules located near corticomedullary junctions. While interstitial edema was not apparent in these sections, medullary sinuses and efferent lymphatics were dilated, suggesting that increased fluid transudation occurred. Numerous mast cells were found randomly dispersed in the capsular, medullary, and hilar regions. While there was no apparent increase in the number or clustering of mast cells in stimulated nodes, more than half of these cells were degranulated at 12 to 48 hours. Free basophilic granules were frequently seen in the tissue surrounding mast cells and within lymph sinuses. However, the "bursting" mast cell degranulation characteristic of antigen–antibody reactions was not observed. This was a transient phenomenon, as normal mast cells were found in all nodes examined at 3 days.

Table 2—Sequential Changes in Regional Nodes Draining Skin Allografts

Days after grafting	Microvascular alterations	Histologic findings
1–2	Contracted venous sphincters, dilated segmental veins, altered vascular permeability	RBCs and PMNs in sinuses, mast cell degranulation, lymphocytic plugging of cortical sinuses
3–7	Dilated cortical capillaries, disappearance of germinal centers, lengthening and arborization HEV	Proliferation of lymphocytes in paracortex, formation of primary follicles, mitotic figures in HEV
14–28	Long arborized HEV persist, avascular nodules in cortex, prominent medullary capillaries	Numerous small lymphocytes in paracortex, large germinal centers, prominent medullary cords

Other findings suggested that lymphocyte traffic was altered in stimulated nodes. Although numerous lymphocytes were seen in the lumens and the walls of HEV in all lymph nodes, observations on random sections suggested that more lympocytes were emigrating into stimulated nodes (Figure 4). Lymphocyte migration indices were employed to estimate the relative rates of lymphocyte entry into these nodes from the bloodstream. The number of migrating lymphocytes and endothelial cells were counted in more than 250 cross sections through HEV in each group. The average lymphocyte migration index was calculated using the formula:

$$\text{Lymphocyte migration index (LMI)} = \frac{\text{number of migrating lymphocytes}}{\text{number of endothelial cells}}$$

There was an abrupt rise in the LMI from control values of 0.75 to 1.28 within 12 hours (Table 3). Increased LMI were observed until 48 hours when they declined towards normal levels.

Over this same time interval (12 to 48 hours), the perivenular sheaths surrounding HEV were packed with small lymphocytes. Tight aggregations of small lymphocytes intermixed with a few macrophages formed cellular plugs which filled intermediate sinus plexuses throughout the cortex (Figure 5). In contrast, the fluid-filled medullary sinuses contained only occasional lymphocytes and macrophages. These changes cleared abruptly by Day 3, when only scattered small lymphocytes were observed in paracortical sinuses.

Table 3—Histologic Signs of Altered Lymphocyte Traffic in Lymph Nodes Draining Skin Allograft Sites

	Histologic findings			
	Regional node		Contralateral node	
Days after grafting	LMI	Lymphocte plugs*	LMI	Lymphocyte plugs*
12 hr	1.28	++	0.75	0
1	1.14	++	0.69	0
2	1.20	+	0.81	0
3	0.84	0	0.68	0
4	0.97	0	0.74	0
7	0.82	0	0.71	0
14	0.81	0	0.68	0
28	0.68	0	0.70	0

Lymphocyte migration index (LMI) = (number of migrating lymphocytes/number of high endothelial cells) × 10.

* Lymphocyte plugs: + = tight aggregates of lymphocytes in cortical sinuses, 0 = individual lymphocytes dispersed in cortical sinuses.

Table 4—Structural Alterations In High Endothelial Venules Within Nodes Draining Skin Allografts

Days after grafting	Average number of high endothelial side branches from each main trunk		Branches lined by high endothelium in cleared slices* (%)	Mean length of high endothelial side branches in cleared slices* (μ)
	Histologic sections	Cleared slices*		
0	2.0	2.1	38	102
1	5.0	1.8	38	134
2	5.8	3.6	52	143
3	7.0	5.0	72	116
4	8.1	7.4	76	142
7	4.0	6.1	81	156
10	—	6.0	96	181
14	1.8	3.1	66	177
28	2.0	2.4	40	128

Vessels lined by four to eight endothelial cells in cross sections were designated *side branches*, and venules lined by 14 or more cells were considered *main HEV trunks*.
*Data derived from direct examination of HEV in cleared slices of nodes perfused with alcian blue *in vivo*.

The first definite signs of enhanced lymphocyte proliferation appeared at 2 days, when occasional large lymphocytes with basophilic cytoplasm were observed in the cortical interstitium surrounding HEV. By 3 to 4 days, the preexisting germinal centers had disappeared, and the paracortex was heavily infiltrated with lymphocytes. Focal collections of small lymphocytes formed primary nodules in the deep cortical zones and numerous large lymphocytes exhibiting basophilic cytoplasm and occasional mitotic figures were dispersed throughout the expanded cortex. By 7 days the number of large lymphocytes in the cortex was decreasing, and several secondary nodules were present. The medullary cords appeared to be wider and contained many plasma cells. From 14 to 28 days the cortex was filled with large germinal centers, and the paracortical zones were populated primarily by small lymphocytes. The prominent medullary cords to plasma cells persisted.

Changes in HEV Within Draining Lymph Nodes

The most striking microvascular changes observed were the apparent lengthening and arborization of HEV in stimulated nodes (Figure 3). In these preparations, the ratio of side branches lined with cuboidal endothelium to main HEV trunks increased from 1.8 on Day 1 to 7.4 on Day 4 (Table 4). This ratio gradually declined to 3.1 by 28 days. In the same nodes, the percentage of HEV side branches lined by high endothelium increased from 38% immediately after grafting to 96% on Day 10 (Table

4). These findings suggested that increased arborization of HEV resulted from the growth of high endothelium into side branches originally lined by low endothelial cells. Direct measurements of side branches lined by high endothelium revealed an increase in mean branch length from 102 μ on Day 1 to 181 μ on Day 10. These findings prompted further attempts to characterize the structural, metabolic, and proliferative changes in these specialized venules.

Histologic Studies of HEV

In toluidine blue-stained thick sections from contralateral nodes, HEV were easily identified by their characteristic metachromatic, polygonal endothelial cell lining and surrounding reticular cell sheath. Numerous small lymphocytes were seen in the lumens, infiltrating the wall and contained within the sheath of these vessels. These multibranched venules originated near the marginal sinus and terminated at the corticomedullary junction. Longitudinal sections through HEV demonstrated that these vessels progressively increased in size as they coursed towards the medulla. Their luminal diameters varied from potential spaces in small side branches to more than 30 μ in terminal segments of the central trunks. The number of endothelial cells seen in cross sections of these venules ranged from four in the small, proximal segments to more than fourteen in dilated segments near the corticomedullary junction. There was an abrupt transition from flat to cuboidal endothelium where small venules joined HEV in the cortex. Occasional mitotic figures were seen in high endothelial cells at these sites in normal and contralateral axillary nodes. A gradual transition from cuboidal to flat endothelium was found at the corticomedullary junction where HEV merged into segmental veins. No mitoses were seen in these transition zones.

The light microscopic appearance of HEV in stimulated nodes was similar to that described above. In addition, increased metachromatic staining of high endothelial cells was apparent in these nodes from Days 3 to 7, but returned to normal levels by 14 to 28 days. Mitotic figures were frequently observed at junctions between high and low endothelial venules from 2 to 7 days after grafting, while no endothelial cell mitoses were found at other sites. Attempts were made to estimate the extent of arborization of HEV in histologic sections of these nodes. Vessels lined by four to eight endothelial cells in cross section were designated as side branches, and venules lined by fourteen or more endothelial cells were considered main trunks of HEV. In contralateral nodes the ratio of side branches to main trunks ranged between 1.7 to 2.5 (Table 4). In

stimulated nodes, this ratio rapidly increased to a peak of 8.1 at 4 days and returned to normal levels by 28 days.

Histochemical Studies of HEV

Cryostat sections from draining and contralateral nodes were stained with histochemical reagents selected to evaluate general and specialized metabolic functions of high endothelial cells. Visual grading of the staining intensity was used to estimate relative metabolic activities in these tissues. The results of these studies are summarized in Text-figure 1. All vascular endothelium in rat lymph nodes stained for adenosine triphosphatase activity (ATPase). HEV in contralateral nodes showed diffuse cytoplasmic ATPase staining of moderate intensity. This metabolic activity increased markedly in high endothelial cells of stimulated nodes within 48 hours after grafting and gradually returned to baseline levels after 7 days. Lactic dehydrogenase (LDH) and isocitric acid dehydrogenase (ICHD) activity was observed in all endothelium, but only high endothelial cells in regional nodes showed transient increases in mitochondrial dehydrogenase staining which persisted for 1 week. While cytoplasmic basophilia was found in the endothelial lining of HEV in control nodes,

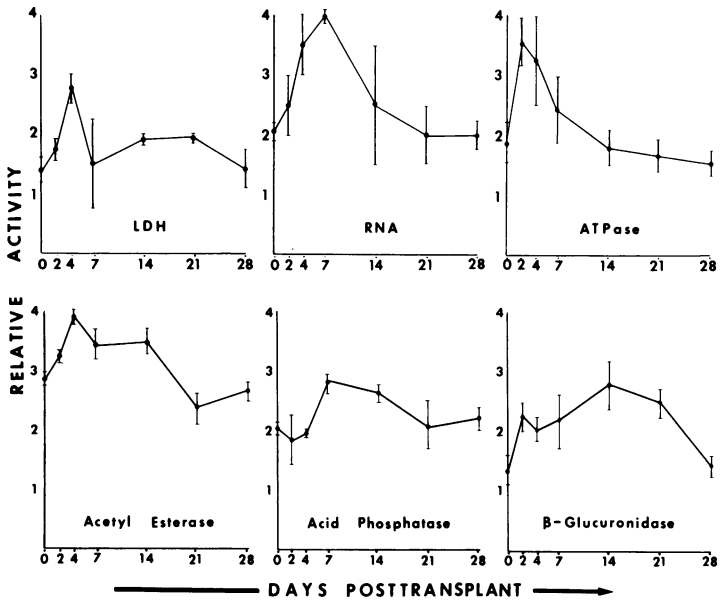

TEXT-FIGURE 1—These graphs illustrate the sequential changes in the metabolic activities of HEV endothelium in regional nodes after skin allografting. Staining intensity was graded on a scale of 0 to 4 within 120 HEV in nodes excised from 4 rats at each time interval. Vertical lines represent the range of metabolic activity seen within individual HEV.

the intensity of this staining reaction was significantly elevated in high endothelial cells within stimulated nodes for 7 days after grafting.

Acetyl esterase and acid hydrolase activities were present in all high endothelial cells, but considerable variations in staining intensity were observed between individual cells within the same venules in normal and stimulated nodes. This variation made it difficult to grade changes in acid hydrolase staining, but there appeared to be a net overall increase in each of these enzymatic activities in stimulated nodes. Esterase and acid phosphatase staining peaked within the first week and then returned to normal levels. β-Glucuronidase activity rapidly increased in stimulated nodes and persisted at relatively high levels for 3 weeks. There were no apparent changes in the distribution of acid hydrolases. The cytoplasm of high endothelial cells always stained diffusely for acid phosphatase and β-gloucuronidase, and the focal granular staining usually associated with phagolysosomes was not seen.

Ultrastructural Changes in HEV Within Draining Nodes

Electron microscopic studies of control axillary nodes showed that all HEV were lined by a continuous monolayer of polygonal endothelial cells (Figure 6). Each cell possessed abundant cytoplasm and measured 10 to 15 μ in height. These cells could be segregated into two distinct morphologic types by differences in cytoplasmic density and cellular organelles. In most endothelial cells the cytoplasm displayed faint electron density and contained numerous free and clustered ribosomes, sparse endoplasmic reticulum, six to eight mitochondria, a prominent Golgi apparatus, occasional pinocytotic vesicles, and two to three residual bodies. The large, lobular nuclei displayed loose chromatin which condensed at the periphery, one to two nucleoli, and ten to twelve nuclear pores. Luminal surfaces of individual cells were usually smooth.

A second population of dark cells was found scattered along the endothelium. The increased cytoplasmic density was due to a marked increase in the number of polyribosomes and rough endoplasmic reticulum (RER). Dense particulate material was seen in RER cisternae; Golgi saccules were dilated. These dark cells contained numerous lysosomes and mitochondria with condensed matrices. Nuclei had irregular borders, 20 to 30 nuclear pores, and nucleoli organized into nucleolonemas. Numerous folds projected from surfaces of these cells into the venular lumen. The ratio of dark to light cells in HEV of the control nodes varied from 0.063 to 0.145. Dark cells were observed in all segments of HEV and typically appeared as individual cells interspersed among group of endothelial cells with light cytoplasm.

Together, these cells formed a continuous endothelial lining. Adjacent cells were linked together by macular tight junctions located near luminal and basal surfaces; overlapping foot processes extended beneath the basilar portion of each cell. The endothelium rested upon a thin basal lamina and was surrounded by a complex, connective tissue sheath composed of two to three layers of overlapping reticular cell plates. Lymphocytes were seen migrating across the wall of all HEV segments in control nodes. While migration in the smaller proximal segments appeared to be confined to single lymphocytes, clusters of two to four lymphocytes were frequently seen migrating through deep clefts between endothelial cells in dilated segments of HEV near the corticomedullary junction. Small lymphocytes were attached to the luminal surfaces of endothelium, between and beneath endothelial cells adjacent to the basal lamina, and within potential spaces between layers of the reticular sheath. All migrating lymphocytes had similar ultrastructural characteristics. They measured 5 to 6 μ in diameter; their pale cytoplasm contained a moderate number of ribosomes and four to five mitrochondria. Nuclei contained compact chromatin which condensed around nucleoli and near the nuclear membrane.

Distinctive ultrastructural changes were observed in HEV of regional nodes draining skin allografts. From 12 to 48 hours after grafting, virtually all high endothelial cells showed increased complexity of the nuclei and more polyribosomes. Macular junctions between adjacent cells remained unaltered in proximal portions of HEV. Focal extravasation of red blood cells was observed in some distal segments where the endothelial lining was disrupted. Numerous macrophages accumulated in the interstitium surrounding these sites and some contained phagocytosed erythrocytes. Increased numbers of lymphocytes were infiltrating the walls of HEV, and clusters of two to four small lymphocytes were frequently seen migrating across mid and distal segments of these venules. There were no apparent changes in the mode of lymphocyte migration from these venules.

At 3 to 4 days after grafting, only occasional endothelial cells displayed light cytoplasm (Figure 7). Most high endothelial cells showed markedly increased numbers of polyribosomes, prominent RER, and early development of RER cisternae. Golgi saccules were dilated, and numerous vesicles were clustered about the concave face. Nuclei contained numerous pores and eccentric, retiform nucleoli. While the extent of the changes varied within individual cells, morphologic signs of endothelial activation were prominent in all HEV. Similar ultrastructural characteristics were observed at 1 week. The cytoplasm of these high endothelial cells was dominated by RER cisternae. Nondilated segments of RER were often ad-

jacent to mitochondrial surfaces. Endothelial cell nuclei showed multiple marginal indentations and 20 to 30 nuclear pores; each nucleolus was organized into a prominent nucleolonema. In addition, the luminal surfaces of many high endothelial cells had ruffled borders with microvillous projections which enveloped membranous and vesicular debris (Figure 7). Phagolysosomes were present in the cytoplasm. Fibrin strands and platelets were occasionally seen in the vascular lumen. Endothelial phagocytosis was seen in all nodes at scattered foci along mid and distal segments of HEV. Membrane folds, phagolysosomes and residual bodies were not observed in proximal portions of HEV lined by four to six endothelial cells in cross section. Mitotic figures were seen in cells which exhibited the cytoplasmic characteristics of high endothelium at sites where the proximal segments merged with low endothelial venules. There were no apparent changes in the sequence of lymphocyte emigration from HEV.

At 14 days, high endothelial cells retained many of the ultrastructural changes noted at 1 week (Figure 8). Most cells appeared "activated," but dilated RER cisternae and Golgi saccules were generally less prominent. Scattered foci of endothelial phagocytosis were observed in many HEV. By 1 month, most HEV were lined by relatively normal appearing endothelial cells which exhibited: light cytoplasm, moderate density of ribosomes, occasional strands of RER, and a prominent Golgi. Varying stages of endothelial cell degeneration were seen in the transition zones from high to low endothelium at corticomedullary junctions. At these sites, cells containing ballooned, vacuolated cytoplasmic organelles, condensed nuclear chromatin, and indistinct cell membranes were interspersed between normal-appearing high and low endothelial cells.

Radiolabeling Studies

Autoradiographic studies were used to determine the rate and sites of endothelial cell proliferation. Since morphologic findings suggested that the venules might proliferate in the first week after stimulation, 4 rats were continuously infused with ^{3}H-thymidine from Days 3 to 6. Serial sections were examined from the draining axillary and contralateral inguinal nodes to compare the effects of regional stimulation on different modes in the same animal (Table 5). Labeled high endothelial cells were observed in all lymph nodes. However, the labeling index of high endothelial cells in stimulated nodes ranged from 8.4 to 13.1% which was approximately six times greater than the 1.9 to 2.2% labeling seen in contralateral nodes. Analysis of serial sections through each node demonstrated that this endothelial cell proliferation was always focal and confined to junctions between HEV and small venules lined with flat endothelium (Figure 9). A

Table 5—Radioautographic Studies of ^{3}H-Thymidine Incorporation by High Endothelial Cells in Lymph Nodes Draining Skin Allografts*

Parameter	Regional axillary nodes (mean ± SD)		Contralateral inguinal nodes (mean ± SD)		$P(\Delta)$
Percent labeled high endothelial cells	13.1	± 2.69	2.2	± 0.36	0.005
Number of consecutively labeled high endothelial cells at transition zones	32.1	± 4.98	30.4	± 3.09	0.20
Percent of transition zones containing labeled high endothelial cells	73.9	± 8.21	12.4	± 7.45	0.0025

* Rats continuously infused with ^{3}H-thymidine from Day 3 to Day 6 after skin grafting.

mean of 32 consecutively labeled, high endothelial cells was found at each transition zone within stimulated and control nodes. The different labeling indices observed in these nodes were clearly related to variations in the number of transition sites engaged in cellular proliferation. In control nodes only 12% of the junctions between high and low endothelium contained labeled cells, while 74% of the transition zones in stimulated nodes from the same rat were labeled by these techniques. No endothelial labeling occurred at transition sites from high to low endothelium in the corticomedullary junction.

Discussion

Early anatomic studies described a rather simplistic microvascular pattern in lymph nodes.[27,28] Arteries entering the hilus were reported to divide into smaller branches which coursed along trabeculae and terminated in medullary cortical capillary beds. These capillaries were thought to empty directly into postcapillary venules which drained into larger veins in the medulla. Although lymph nodes were recognized as actively metabolizing tissues which rapidly enlarged to two to five times their original weight after antigenic challenge,[29] there has been prolonged debate over the nature of the vascular changes within stimulated nodes. Several investigators suggested that the cortical vasculature might be remodeled as germinal centers waxed and waned in the cortex.[7,8] This thesis was substantiated by Dabelow's perfusion studies of regional nodes stimulated by heat-killed bacteria,[30] which demonstrated that enlarging germinal centers displaced adjacent capillaries and arteriovenous communications in the adjacent cortex. Suggestions that blood vessels might proliferate in antigen-stimulated nodes have never been adequately documented.[11-13] Recently, Herman *et al.*[10] employed microangiographic

techniques to study the microvasculature in rabbit popliteal lymph nodes challenged with *Salmonella* 0 antigen. They described an early phase of vasodilatation which was attributed to acute inflammation. This was followed by complete dissolution of the vascular units within cortical lobules and increased vascularity of the medullary cords at 2 to 4 days. However, avascular germinal centers rapidly reformed in these nodes and the microvascular pattern returned to normal within 7 days. These investigators concluded that variations in the angioarchitecture resulted from redistribution of existing vessels, since no changes suggestive of neovascularization were observed. Capillaries maintained their regular outlines, and the number of HEV did not change significantly.

The present study provided additional information on changes in microvasculature of stimulated lymph nodes. From 12 to 48 hours, all regional nodes showed dilated cortical capillary arcades and diffuse staining of reticular fibers by intraarterially infused dye. These findings were entirely consistent with the altered vascular permeability which other investigators [6] have attributed to inflammatory changes produced by antigenic challenge. The presence of numerous, dilated arteriovenous communications suggested increased shunting of arterial blood into nodal veins where contracted venous sphincters appeared to increase resistance to venous flow and dilate segmental veins. Our histologic studies indicated that this sequence of events was occasionally accompanied by spontaneous extravasation of blood at corticomedullary junctions where HEV merged with segmental veins. The temporal association between these findings and the diffusion of alcian blue dye from nodal vessels suggested that elevated venous pressure contributed to fluid transudation. Since signifiant interstitial edema was not seen in histologic sections, this fluid transudation probably added to the elevated lymph output which has been observed by cannulating efferent lymphatics of stimulated nodes.[31] This specialized microvasculature clearly provided a unique system for redistributing and regulating blood flow in the early stages after antigenic challenge. Previous studies demonstrated arteriovenous communications and venous sphincters that were innervated by unmyelinated nerve fibers and contracted following regional infusions with catecholamines.[19] While the presence of degranulated mast cells in these nodes suggested that local histamine release affected vascular permeability, further studies will be required to determine the responses of this vascular bed to other vasoactive agents which may be liberated during immune reactions.

In regional nodes, these microvascular changes were accompanied by signs of altered lymphocyte traffic which persisted for about 48 hours. Several reports attributed the initial increases in weight and cellularity of

stimulated nodes to recruitment of lymphocytes from the circulation.[4,32] Other studies demonstrated increased accumulation of transfused radiolabeled lymphocytes within draining lymph nodes for 1 to 2 days following local injections of antigen or particulate materials.[33,34] This process of "lymphocyte-trapping" was associated with the appearance of compact, cellular aggregates in cortical sinuses. It has been suggested that increased surface adherence between lympocytes and activated macrophages resulted in the formation of cellular plugs which occluded narrow lymph sinuses and blocked the entry of lymphocytes into efferent lymphatics.[36] Similar histologic findings were observed within nodes draining allografts in this study. Zatz and Lance [34] postulated that this trapping phenomenon might include increased cellular traffic into the node which could not be demonstrated by simply measuring the accumulation of radiolabeled cells. In the present study, increased numbers of migrating lymphocytes were found infiltrating the walls of HEV in stimulated nodes. Attempts to quantitate this process showed that the lymphocyte migration index in regional nodes was nearly twice as great as that seen in contralateral nodes from 12 to 48 hours. Since there were no apparent changes in the size and number of HEV or the mode of cellular migration, these histologic findings provided evidence for increased lymphocyte traffic into regional nodes over this time interval. Lymphocyte migration indices returned to normal levels at later stages, but this probably did not accurately reflect total cellular traffic into the nodes where HEV showed increased length and arborization.

Contracted venous sphincters, dilated veins, and signs of altered vascular permeability were rarely seen at 3 to 4 days. However, striking microvascular changes were found in the cortices. No germinal centers were seen, and rich capillary arcades were evenly distributed throughout the widened cortex. This was paralleled by the appearance of numerous medium, large, and pyroninophilic lymphocytes in the cortex, as noted by other investigators.[11,12,35,37] Small, primary nodules formed in the cortex and were surrounded by glomerulus-like capillary tufts. These nodules evolved into typical germinal centers by 7 to 14 days. As these relatively avascular follicles expanded, they displaced adjacent cortical capillaries, and the vascular pattern assumed a relatively normal appearance. Over the same interval, dilated capillary arcades were found in widened medullary cords populated with plasma cells. All of these changes could be explained by redistribution of blood flow and reorganization of existing blood vessels, as suggested by Herman *et al.*[10] Label was not seen over capillary endothelial cells in autoradiographs of regional nodes from rats infused with ^{3}H-thymidine. However, the findings did not exclude

neovascularization, since it was difficult to identify small blood vessels in these tissue sections. Further studies will be required to determine whether capillary proliferation occurs in stimulated nodes.

Previous reports described occasional mitotic figures in high endothelial cells within normal lymph nodes.[11,14,15] Since intermittent infusions with ^{3}H-thymidine labeled few high endothelial cells, this endothelium was thought to exhibit slow turnover times, with life-spans exceeding 100 days.[16] Burwell [11] suggested that HEV proliferated in nodes subjected to antigenic stimulation, but other investigators found no evidence for such changes.[10,15] Definite signs of endothelial cell proliferation were observed in HEV in the present study. Examination of cleared tissue slices showed progressive lengthening and arborization of HEV branches between Days 3 and 7. This interpretation was supported by histologic sections which increased numbers of small and medium-sized HEV and relatively frequent mitotic figures in high endothelial cells over the same time span. Autoradiographic studies of nodes from animals continually infused with ^{3}H-thymidine for 3 days provided conclusive evidence of endothelial proliferation. Numerous labeled high endothelial cells were found in stimulated nodes, and this labeling was restricted to transition zones from high to low endothelium in the outer cortex. About 75% of the zones were labeled in stimulated nodes; examination of serial sections showed a mean of 32 consecutively labeled high endothelial cells at each of these sites. Relatively few foci of labeled high endothelial cells were seen in contralateral nodes, and these were usually concentrated in one or two cortical lobules which represent the drainage area of a single afferent lymphatic.[36] Approximately 30 consecutively labeled high endothelial cells were found in each of the transition zones. These findings indicated that high endothelial venules proliferated during immune reactions. Similar rates of endothelial proliferation were observed within individual venules from nodes subjected to different antigenic stimuli. The striking difference between the number of proliferating HEV in regional and contralateral nodes suggested that this process may be related to the distribution, intensity and duration of antigenic stimulation within individual nodes. The focal nature of the proliferation and its association with antigenic challenge probably explains why this cellular replication has been overlooked previously.

Electron microscopic studies revealed mitotic figures within cells which displayed the typical ultrastructural characteristics of high endothelium. Since there was no evidence of proliferation and differentiation of flat endothelium in these vessels, the findings suggested that growth of HEV was dependent upon replication of high endothelial cells in transition zones.

No attempts were made to estimate the life span and ultimate fate of labeled endothelial cells. However, microscopic studies of cleared sections suggested that high endothelial cells gradually replaced low endothelium in all side branches of HEV within stimulated nodes. No further lengthening of these venous segments was seen after 14 days; by 28 days many side branches contained slightly shorter segments of high endothelium surrounding relatively large lumens. Examination of contralateral nodes showed a gradual transition from high to low endothelium at the corticomedullary junction which differed from the abrupt transition zones seen in the outer cortex. Ultrastructural studies of nodes excised at 1 month demonstrated definite degenerative changes in high endothelial cells. The sequential changes observed in HEV suggested that the specialized endothelium in these vessels may proliferate at its proximal portions and undergo regressive changes distally in the medulla. The net result of this process could be a gradual, intermittent centrifugal movement of HEV away from the medulla as nodes are subjected to repetitive antigenic stimulation.

Previous studies [38] demonstrated that high endothelial cells possessed distinctive metabolic characteristics which were altered in antigen-stimulated nodes. Burwell [11] described increased cytoplasmic basophilia in HEV within regional nodes draining bone allografts and suggested that these cells were engaged in antigen transport. The acid hydrolase activity found within high endothelial cells in normal nodes has been correlated with the presence of a prominent Golgi apparatus,[16] but increases in this activity following regional injections with typhoid vaccine were attributed to the appearance of lysosomes within the cells.[39] In the present experiments, definite metabolic changes were seen in HEV within stimulated nodes. The transient increases in LDH and ICDH levels were probably related to accentuated respiratory activity. The increased cytoplasmic basophilia correlated with the ultrastructural demonstration of numerous polysomes in high endothelial cells. Increased ATPase staining was observed in these cells, but the function of the enzymatic activity remains uncertain. There was a temporal association between these changes of endothelial "activation" and altered fluid and cellular transport, but the precise relations between the events were not established. Modest elevations of nonspecific esterase and acid hydrolase activities were seen in high endothelial cells at later stages after grafting; this appeared to correlate with the ultrastructural demonstration of endothelial phagocytosis in the HEV.

Several descriptions of the ultrastructural characteristics of high endothelial cells have been reported.[40-43] Most of these studies described a

relatively constant morphology in this endothelium where individual cells contained: numerous ribosomes, scant RER, several mitochondria, well-developed Golgi complexes, and a few dense bodies. The present study and related reports from this laboratory indicated that HEV in normal and contralateral lymph nodes were populated predominantly by endothelial cells with these ultrastructural features. In addition, occasional cells exhibiting numerous polyribosomes, RER cisternae, and nuclear changes indicative of increased RNA and protein synthesis were seen. These cells clearly differed from the "dark cells" exhibiting advanced degenerative changes which have been described in other types of endothelia.[44] The ultrastructural appearance of the endothelium was markedly altered by skin grafting. Increased numbers of polyribosomes were seen within 12 to 14 hours; between 3 and 14 days virtually all high endothelial cells exhibited cytoplasmic organelle and nuclear changes consistent with enhanced RNA and protein synthesis. The functional significance of this endothelial "activation" in stimulated nodes remains uncertain. These changes peaked after signs of inflammation and increased lymphocyte traffic into the node had resolved. Since "activated" endothelial cells were seen in all segments of HEV, it seemed unlikely that these changes were related to the focal cellular proliferation occurring in transition zones. Jorgensen and Claësson [45] described similar changes in HEV of neonatally thymectomized mice and suggested that these alterations represented progressive endothelial cell degeneration associated with wasting disease. While some form of diffuse endothelial injury might have produced these changes in stimulated nodes, these cells did not undergo progressive degeneration. By 28 days after grafting, most HEV displayed a relatively normal appearance, and focal endothelial degeneration was observed only at junctions with segmental veins in the medulla. Activated endothelial cells were seen phagocytosing cellular debris and fibrin strands from the vascular lumen at 7 to 14 days. This process was usually observed at scattered foci where microthrombi formed in HEV, but many high endothelial cells at other sites contained increased numbers of lysosomes. Phagocytosis was the only specialized function which could be directly correlated with signs of endothelial activation in this study. While previous studies [46] demonstrated that high endothelial cells ingested and degraded a variety of different agents infused into the regional circulation, signs of spontaneous phagocytosis were seen infrequently in normal nodes. The present study clearly indicated that endothelial phagocytosis was markedly increased in stimulated nodes. This increase might reflect the ingestion of cellular debris released into the bloodstream during lymph node remodeling. However, there is evidence that a variety of

different lymphokines, inflammatory products, antigen–antibody complexes, and activated complement components may be produced in antigen-stimulated nodes.[31,36,47] Since the walls of HEV serve as functional lymph node–venous communications,[48] these products may directly activate high endothelial cells or cause local intravascular clotting which induces endothelial phagocytosis. The latter mechanism seems particularly attractive in view of the association between microthrombi and endothelial phagocytosis observed in the present study.

References

1. Osogoe B, Courtice FC: The effects of occlusion of the blood supply to the popliteal lymph node of the rabbit on the cell and protein content of the lymph and on the histology of the node. Aust J Exp Biol Med Sci 46:515–524, 1968
2. Gowans JL, Knight EJ: The route of re-circulation of lymphocytes in the rat. Proc R Soc Lond [Biol] 159:257–282, 1964
3. Ehrich WE, Harris TN: The formation of antibodies in the popliteal lymph node in rabbits. J Exp Med 76:335–348, 1942
4. Taub RN, Gershon RK: The effect of localized injection of adjuvant material on the draining lymph node. III. Thymus dependence. J Immunol 108:377–386, 1972
5. Gyllensten L, Ringertz N, Ringertz NR: The uptake of labelled phosphate in lymph nodes during experimental lymphadenitis in relation to the morphological picture. Acta Pathol Microbiol Scand 38:81–95, 1956
6. Ringertz N, Adamson CA: The lymph-node response to various antigens: An experimental-morphological study. Acta Pathol Microbiol Scand 27(Suppl 86):1–69, 1950
7. Conway EA: Cyclic changes in lymphatic nodules. Anat Rec 69:487–513, 1937
8. Kojima M, Takahashi K, Sue A, Imai Y: Study on the function and structure of blood vessels of the secondary nodules in lymph node. Acta Pathol Jap 21:369–386, 1971
9. Sainte-Maire G, Sin YM: The lymph node. Structures and possible function during the immune response. Regulation of Hematopoiesis. Edited by AS Gordon. New York, Appleton-Century-Crofts, 1970, p 1340
10. Herman PG, Yamamoto I, Mellins HZ: Blood microcirculation in the lymph node during the primary immune response. J Exp Med 136:697–714, 1972
11. Burwell RG: Studies of the primary and the secondary immune responses of lymph nodes draining homografts of fresh cancellous bone (with particular reference to mechanisms of lymph node reactivity). Ann NY Acad Sci 99:821–860, 1962
12. Parrott DMV, de Sousa MAB: Changes in the thymus-dependent areas of lymph nodes after immunological stimulation. Nature 212:1316–1317, 1966
13. Borum K, Claësson MH: Histology of the induction phase of the primary immune response in lymph nodes of germfree mice. Acta Pathol Microbiol Scand [A] 79:561–568, 1971
14. Hummel KP: The structure and development of the lymphatic tissue in the intestine of the albino rat. Am J Anat 57:351–383, 1935
15. Krüger G: Morphology of postcapillary venules under different experimental conditions. J Natl Cancer Inst 41:287–301, 1968
16. Röpke C, Jorgensen O, Claësson MH: Histochemical studies of high-endothelial venules of lymph nodes and Peyer's patches in the mouse. Z Zellforsch Mikrosk Anat 131:287–297, 1972
17. Billingham RE: Free skin grafting in mammals. Transplantation of Tissues and

Cells. Edited by RE Billingham, WK Silvers. Philadelphia, Wistar Institute Press, 1961, p 1
18. Billingham RE, Hodge BA, Silvers WK: An estimate of the number of histocompatibility loci in the rat. Proc Natl Acad Sci USA 48:138–147, 1962
19. Anderson AO, Anderson ND, Wyllie RG: Morphologic studies on lymph node vasculature. Am J Pathol 74:54a, 1974 (Abstr)
20. Barka T, Anderson PJ: Histochemistry. New York, Harper and Row, 1963, p 314
21. Wyllie RG: Unpublished data
22. Wachstein M, Meisel E: Histochemistry of hepatic phosphatases at a physiologic pH; with special reference to the demonstration of bile canaliculi. Am J Clin Pathol 27:13–23, 1957
23. Davis BJ, Ornstein L: High resolution enzyme localization with a new diazo reagent, "hemazonium pararosaniline." J Histochem Cytochem 7:297–298, 1959 (Abstr)
24. Barka T: A simple azo-dye method for histochemical demonstration of acid phosphatase. Nature 187:248–249, 1960
25. Hayashi M, Nakajima Y, Fishman WH: The cytologic demonstration of β-glucuronidase employing naphthol AS-BI glucuronide and hexazonium pararosanilin: A preliminary report. J Histochem Cytochem 12:293–297, 1964
26. Gomori G: Aldehyde-fuchsin: A new stain for elastic tissue. Am J Clin Pathol 20: 665–666, 1950
27. Calvert WJ: The blood-vessels of the lymphatic gland. Anat Anz 13:174–180, 1897
28. Maximow A: Bindegewebe und blutbildende Gewebe. Handbuch der normalen mikroskopischen Anatomie des Menschen, Vol II/I. Berlin, Springer, 1927, p 232
29. Victor J: The metabolism of single normal mouse lymph nodes. Am J Physiol 111:477–482, 1935
30. Dabelow A: Die Blutversorgung der lymphatischen Organen. Anat Anz 87:179–224, 1939
31. Hall JG: Studies of the cells in the afferent and efferent lymph of lymph nodes draining the site of skin homografts. J Exp Med 125:737–754, 1967
32. Nossal GJV, Mäkelä O: Autoradiographic studies on the immune response. I. The kinetics of plasma cell proliferation. J Exp Med 115:209–230, 1962
33. Dresser DW, Taub RN, Krantz AR: The effect of localized injection of adjuvant material on the draining lymph node. II. Circulating lymphocytes. Immunology 18:663–670, 1970
34. Zatz MM, Lance EM: The distribution of ^{51}Cr-labeled lymphocytes into antigen-stimulated mice: Lymphocyte trapping. J Exp Med 134:224–241, 1971
35. de Sousa MAB, Parrott DMV: Induction and recall in contact sensitivity: Changes in skin and draining lymph nodes of intact and thymectomized mice. J Exp Med 130:671–690, 1969
36. Kelly RH, Wolstencroft RA, Dumonde DC, Balfour BM: Role of lymphocyte activation products (LAP) in cell-mediated immunity. II. Effects of lymphocyte activation products on lymph node architecture and evidence for peripheral release of LAP following antigenic stimulation. Clin Exp Immunol 10:49–64, 1972
37. Scothorne RJ, McGregor IA: Cellular changes in lymph nodes and spleen following skin homografting in the rabbit. J Anat 89:283–292, 1955
38. Smith C, Henon BK: Histological and histochemical study of high endothelium of post-capillary veins of the lymph node. Anat Rec 135:297–213, 1959
39. Mikata A, Niki R, Watanabe S: Reticulo-endothelial system of the lymph node parenchyma, with special reference to post-capillary venules and granuloma formation. Recent Adv RES Res 8:143–154, 1968
40. Clark SL, Jr: The reticulum of lymph nodes in mice studied with the electron microscope. Am J Anat 110:217–257, 1962

41. Marchesi VT, Gowans JL: The migration of lymphocytes through the endothelium of venules in lymph nodes: An electron microscope study. Proc R Soc Lond [Biol] 159:283–290, 1964
42. Sugimura M: Fine structure of post-capillary venules in mouse lymph nodes. Jap J Vet Rest 12:83–90, 1964
43. Claesson MH, Jorgensen O, Röpke C: Light and electron microscopic studies of the paracortical post-capillary high-endothelial venules. Z Zellforsch Mikrosk Anat 119:195–207, 1971
44. Steiner JW, Carruthers JS, Kalifat SR: Vascular alterations in the liver of rats with extrahepatic biliary obstruction: An electron and fluorescent microscopic study. Exp Mol Pathol 1:427–456, 1962
45. Jorgensen O, Claesson MH: Studies on the post-capillary high endothelial venules of neonatally thymectomized mice. A Zellforsch Mikrosk Anat 132:347–355, 1972
46. Anderson AO, Wyllie RG, Anderson ND: Structural, metabolic and functional characteristics of post-capillary venular (PCV) endothelium in rat lymph nodes. Fed Proc 32:861abs, 1973
47. Willoughby DA, Boughton B, Schild HO: A factor capable of increasing vascular permeability present in lymph node cells: A possible mediator of the delayed reaction. Immunology 6:484–498, 1963
48. Anderson AO, Anderson ND, Wyllie RG: Lymphocyte emigration from high endothelial venules (HEV). Fed Proc 33:628 (abstr), 1974

[*Illustrations follow*]

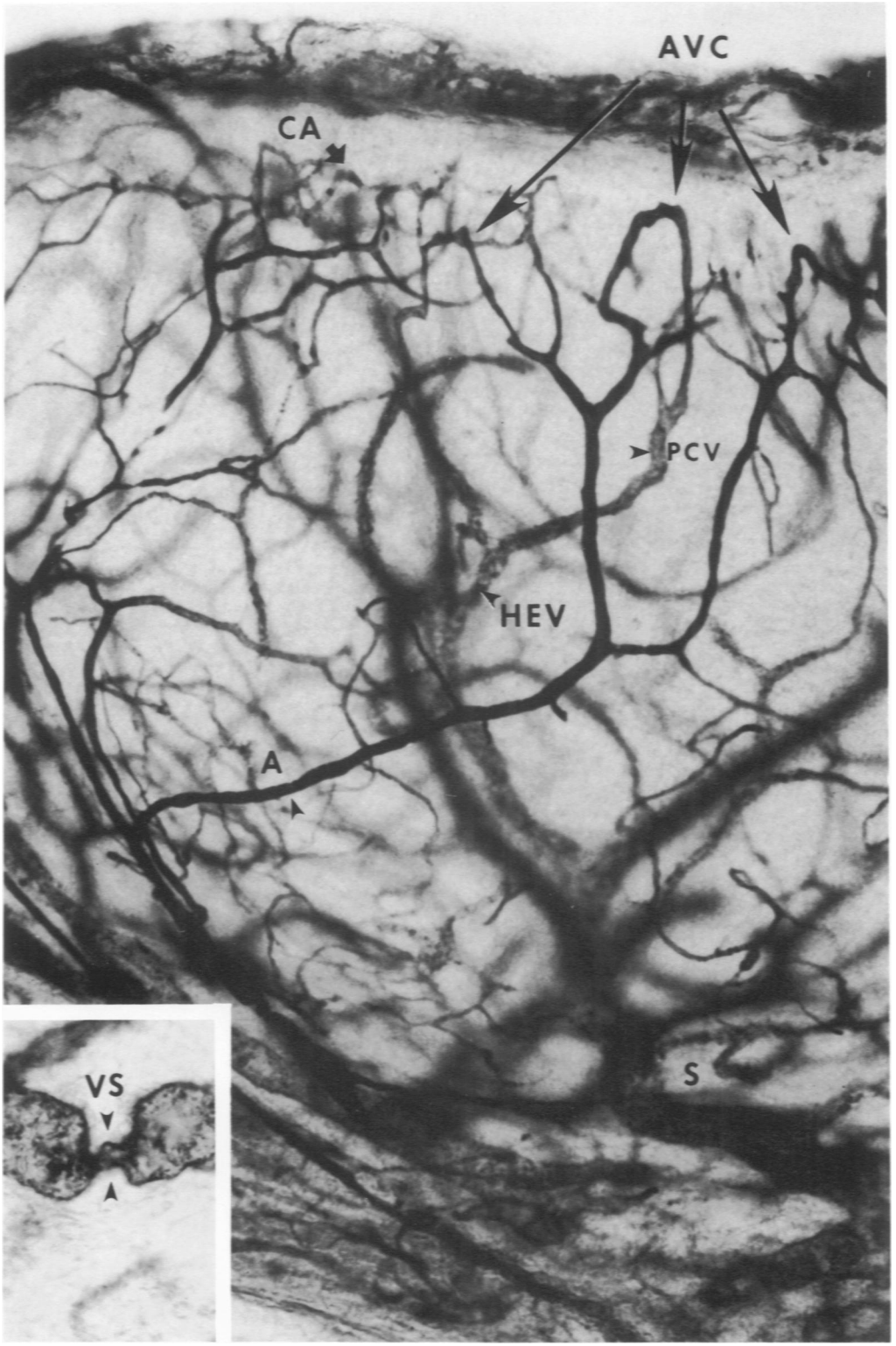

Figure 1—Microvasculature in a 150-μ, cleared section from a control axillary node perfused *in vivo* with alcian blue dye. *A* = segmental artery, *CA* = capillary arcade, *AVC* = arteriovenous communication, *PCV* = postcapillary venule, *HEV* = high endothelial venule, *S* = segmental vein. (× 160) **Inset**-Venous sphincter (*VS*) in a segmental vein near the hilus is shown (× 330).

Figure 2—In this regional node excised 3 days after grafting, high endothelial venules (HEV) appear vertically oriented. High endothelial side branches (*arrows*) are linked to the capillary bed by short postcapillary venules (*PCV*) lined with flat endothelium. Staining of reticular fibers (*RF*) after extraarterial perfusion with alcian blue indicates increased permeability of cortical vessels. (× 160)

Figure 3—Typical appearance of HEV in cleared section from a regional node at 7 days postgrafting. Most of the side branches (*arrows*) are lined by cuboidal endothelial cells. (× 190)

Figure 4—Numerous lymphocytes are seen within the lumen (*a*), in the wall (*b*), and traversing the reticular cell sheath (*c*) of this HEV in a regional node excised 24 hours after grafting (Toluidine blue, × 925).

Figure 5—Lymphocyte "plugs" within a distended intermediate sinus (*IS*) in a regional node at 24 hours after grafting (H&E, × 225).

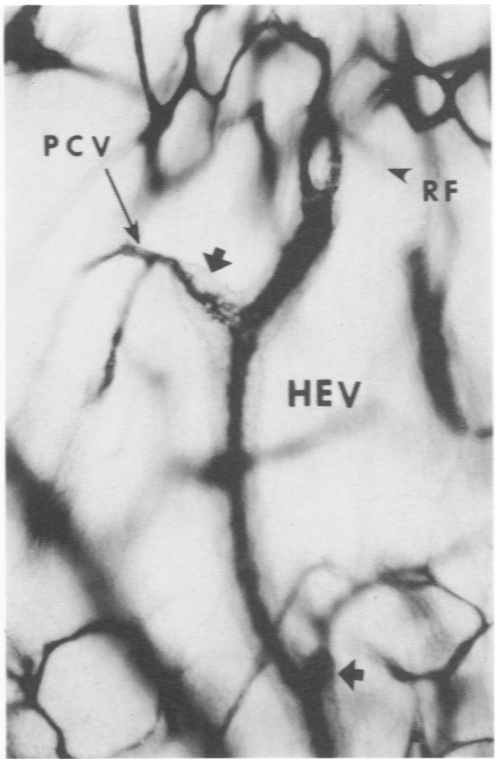

2

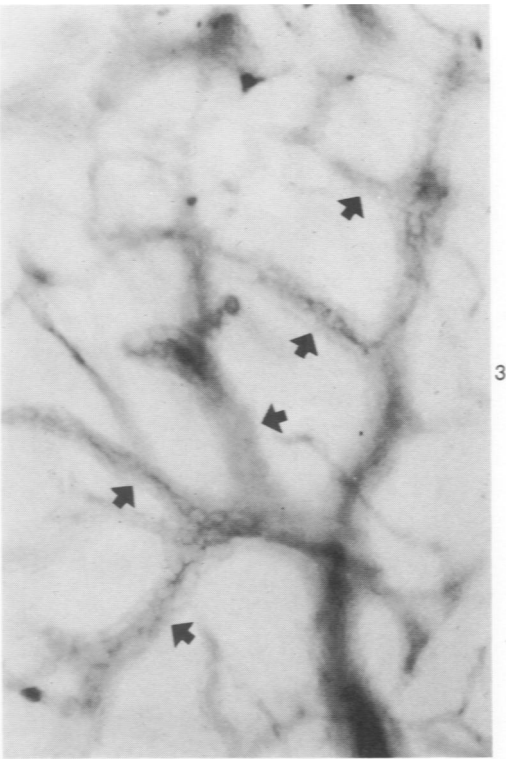

3

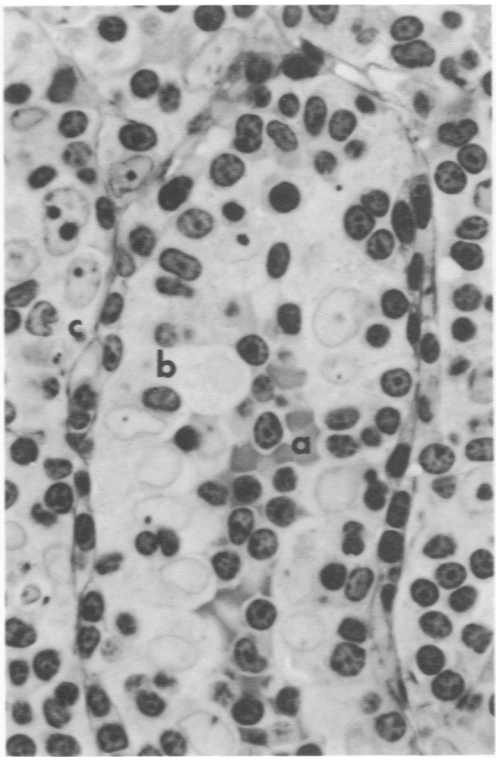

4

5

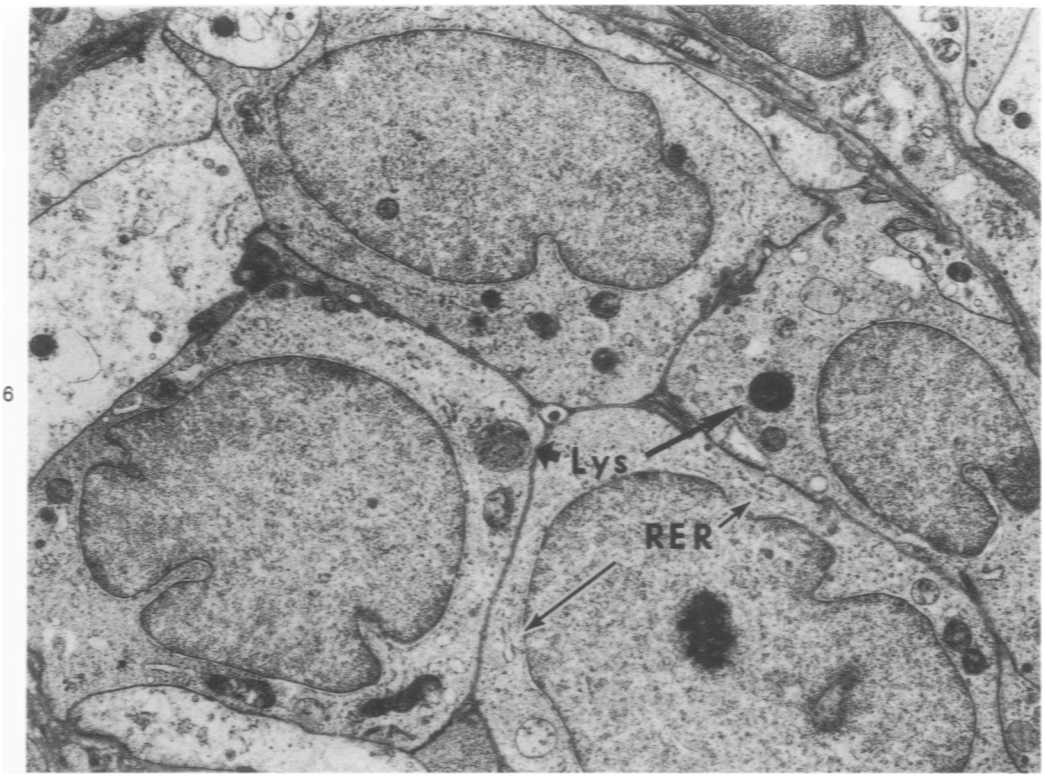

6

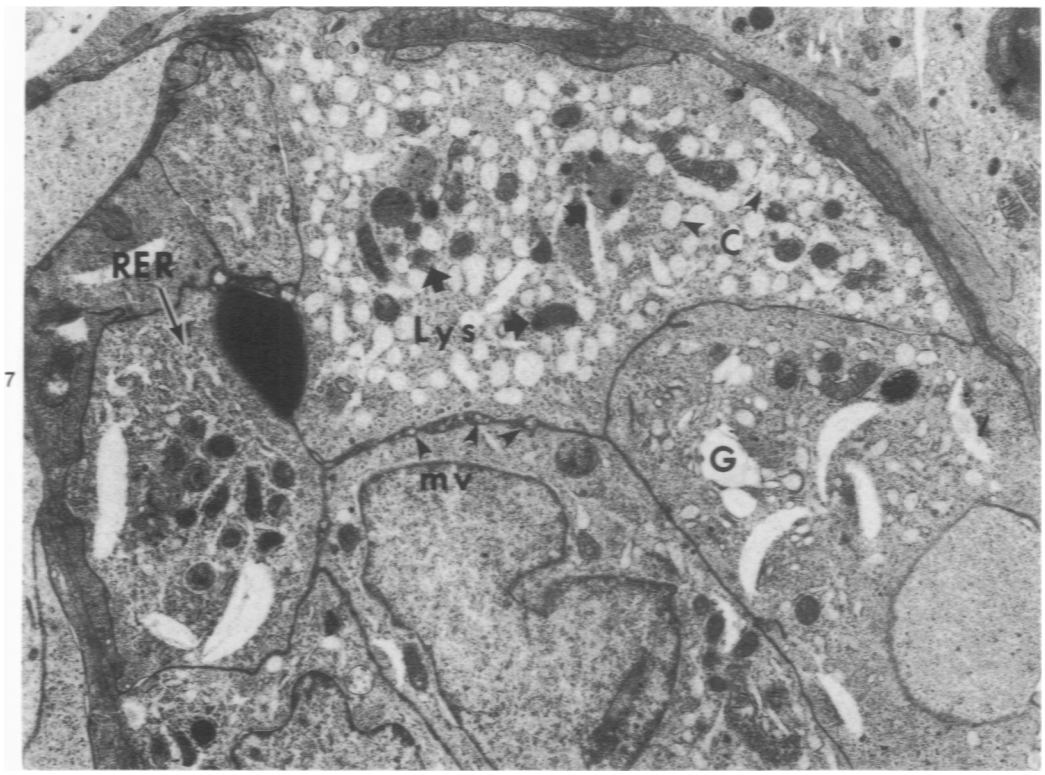

7

Figure 6—This electron micrograph shows the typical appearance of high endothelial cells in control nodes. The abundant cytoplasm of the cells exhibits faint electron density and contains ribosomes, mitochondria, lysosomes (*Lys*), and sparse rough endoplasmic reticulum (*RER*). (× 8000)
Figure 7—At 3 days postgrafting, HEV contain numerous "activated" endothelial cells. These cells exhibit: increased ribosomal density, abundant rough endoplasmic reticulum with cysternae (*C*), distended Golgi (*G*), prominent lysosomes (*Lys*), and microvilli (*Mv*) on their luminal surfaces. (× 8000)

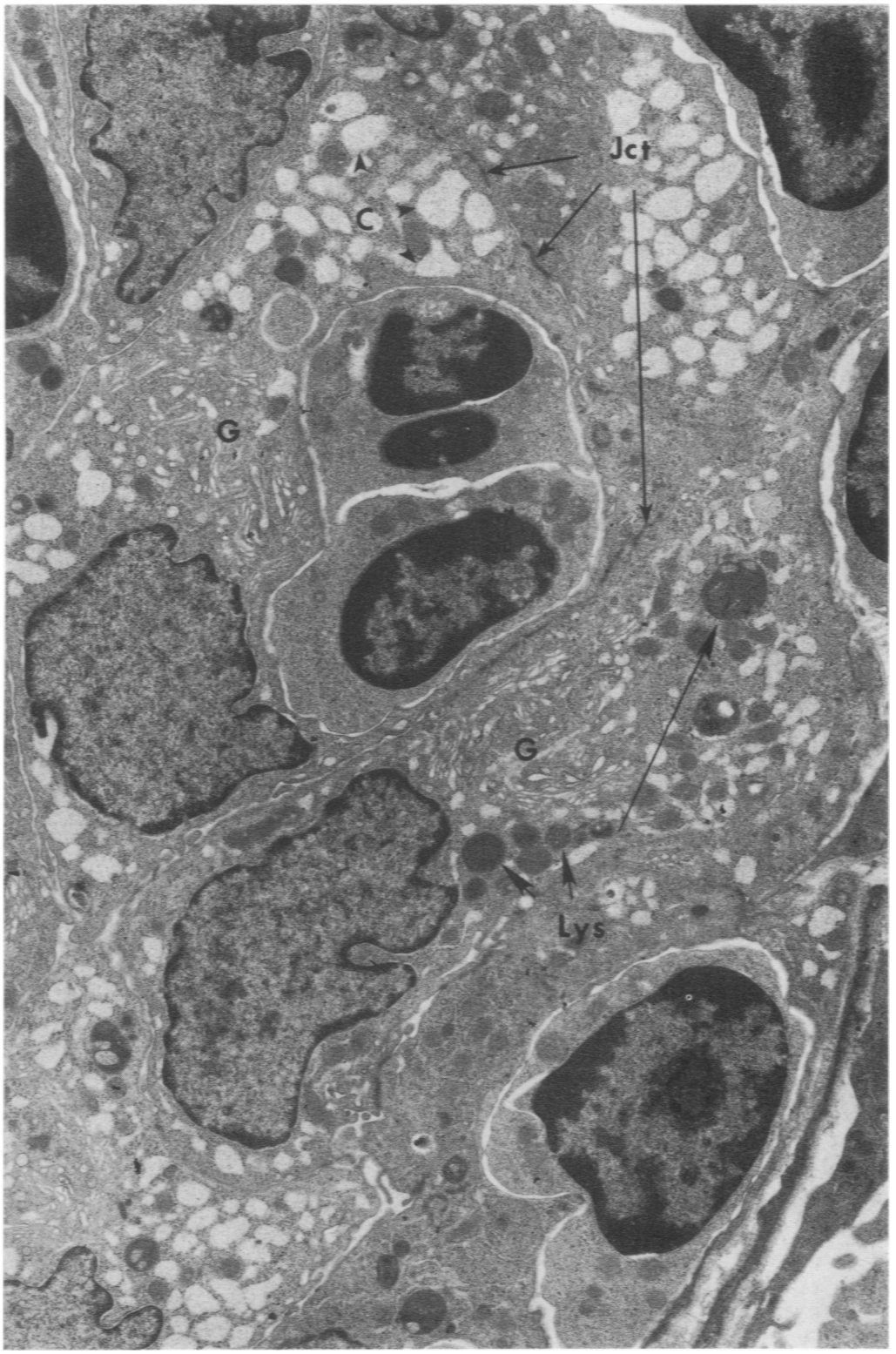

Figure 8—Morphologic changes of endothelial "activation" persist at 14 days after grafting. These endothelial cells contain prominent Golgi (*G*) and numerous lysosomes (*Lys*). The rough endoplasmic reticulum is almost entirely composed of cysternae (*C*). This plane of sectioning illustrates the polygonal endothelial cell contours and discontinuous junctions (*Jct*) between adjacent cells. (× 8100)

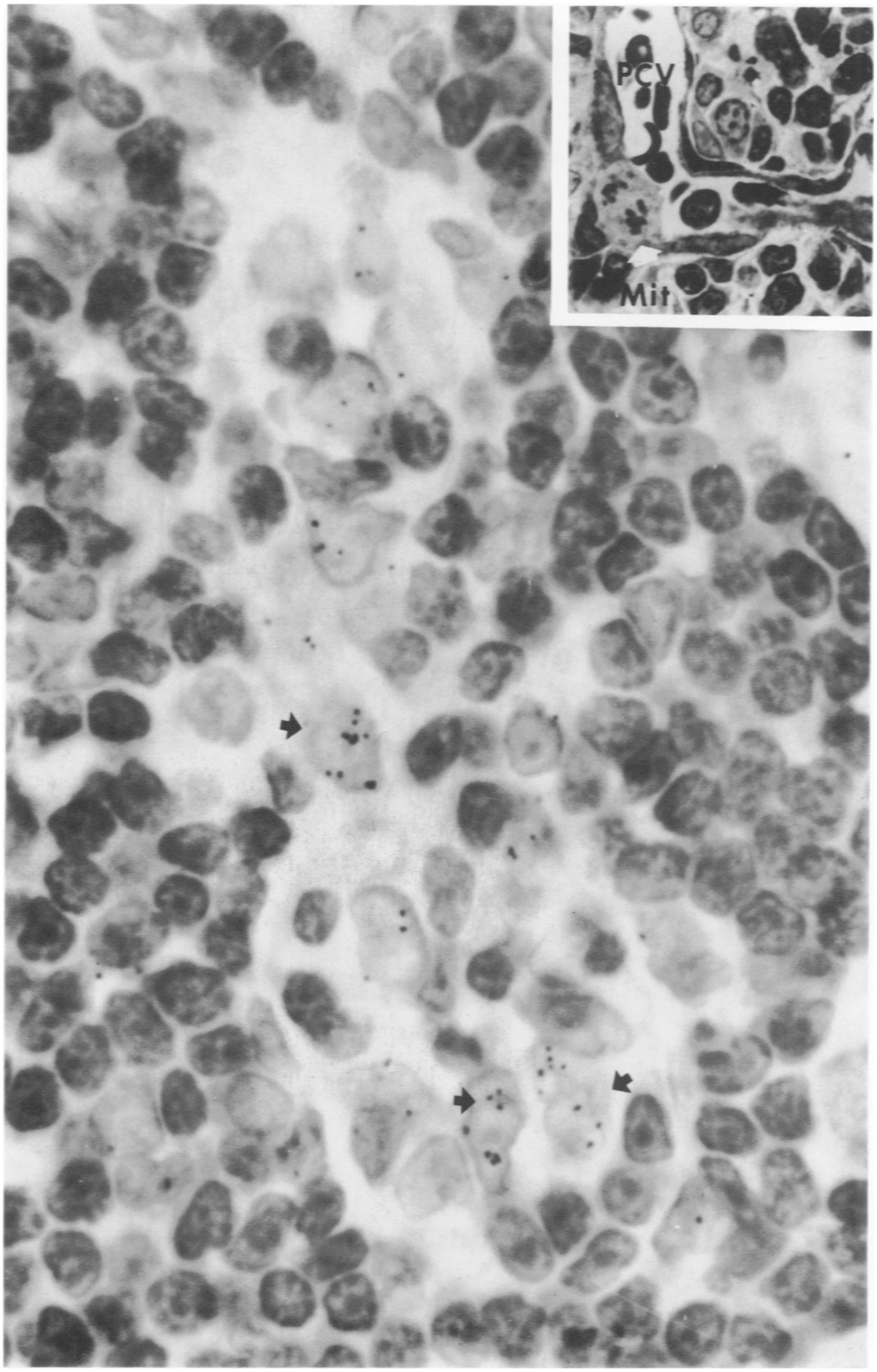

Figure 9—Continuous infusion with ^{3}H-thymidine from the third to the sixth day after grafting resulted in nuclear labeling (*arrows*) of a series of high endothelial cells at junctions between HEV and postcapillary venules (*PCV*) lined by low endothelium (H&E, × 2200). **Inset**—Mitotic figures were frequently seen at these sites (Toluidine blue, × 1200).